Bulletin of the Seismological Society of America, Vol. 97, No. 5, pp. 1379–1395, October 2007, doi: 10.1785/0120060267

Review Article

Topographic Slope as a Proxy for Seismic Site Conditions and Amplification

by David J. Wald and Trevor I. Allen

Abstract We describe a technique to derive first-order site-condition maps directly from topographic data. For calibration, we use global 30 arc sec topographic data and V_S^{30} measurements (here V_S^{30} refers to the average shear-velocity down to 30 m) aggregated from several studies in the United States, as well as in Taiwan, Italy, and Australia. V_S^{30} values are correlated against topographic slope to develop two sets of parameters for deriving V_S^{30}: one for active tectonic regions where topographic relief is high, and one for stable shields where topography is more subdued. By taking the gradient of the topography and choosing ranges of slope that maximize the correlation with shallow shear-velocity observations, we can recover, to first order, many of the spatially varying features of site-condition maps developed for California. Our site-condition map for the low-relief Mississippi Embayment also predicts the bulk of the V_S^{30} observations in that region despite rather low slope ranges.

We find that maps derived from the slope of the topography are often well correlated with other independently derived, regional-scale site-condition maps, but the latter maps vary in quality and continuity, and subsequently, also in their ability to match observed V_S^{30} measurements contained therein. Alternatively, the slope-based method provides a simple approach to uniform site-condition mapping.

After validating this approach in regions with numerous V_S^{30} observations, we subsequently estimate and map site conditions for the entire continental United States using the respective slope correlations.

Introduction

Recognition of the importance of the ground-motion amplification from regolith has led to the development of systematic approaches to mapping seismic site conditions (e.g., Park and Elrick, 1998; Wills *et al.*, 2000; Holzer *et al.*, 2005) as well as quantifying both amplitude- and frequency-dependent site amplification (e.g., Borcherdt, 1994). A now standardized approach for mapping seismic site conditions is measuring or mapping V_S^{30}. In fact, many U.S. Building codes now require site characterization explicitly as V_S^{30} (e.g., Dobry *et al.*, 2000; Building Seismic Safety Council [BSSC], 2000, 2004). In addition, many of the ground-motion prediction equations (e.g., Boore *et al.*, 1997; Chiou and Youngs, 2006) are calibrated against seismic station site conditions described with V_S^{30} values.

Maps of seismic site conditions on regional scales are not always available because they require substantial investment in geological and geotechnical data acquisition as well as interpretation. In many seismically active regions of the world, information about surficial geology and shear-wave velocity (V_S) either does not exist, varies dramatically in quality, varies spatially, or is not easily accessible. Such maps are available for only a few regions, predominantly for seismically active urban areas of the world. Topographic elevation data, on the other hand, are available at uniform sampling for the globe. Intuitively, topographic variations should be an indicator of near-surface geomorphology and lithology to the first order, with steep mountains indicating rock, nearly flat basins indicating soil, and a transition between the end members on intermediate slopes. Indeed, the similarity between the topography of California (Fig. 1a) and the surficial site-condition map derived from geology (Fig. 1b) is striking. In addition, recent studies have confirmed good correlations between V_S^{30} and both slope and geomorphic indicators in Japan (e.g., Matsuoka *et al.*, 2005) and elevation with V_S^{30} in Taiwan (e.g., Chiou and Youngs, 2006). Other geoscience disciplines have used similar

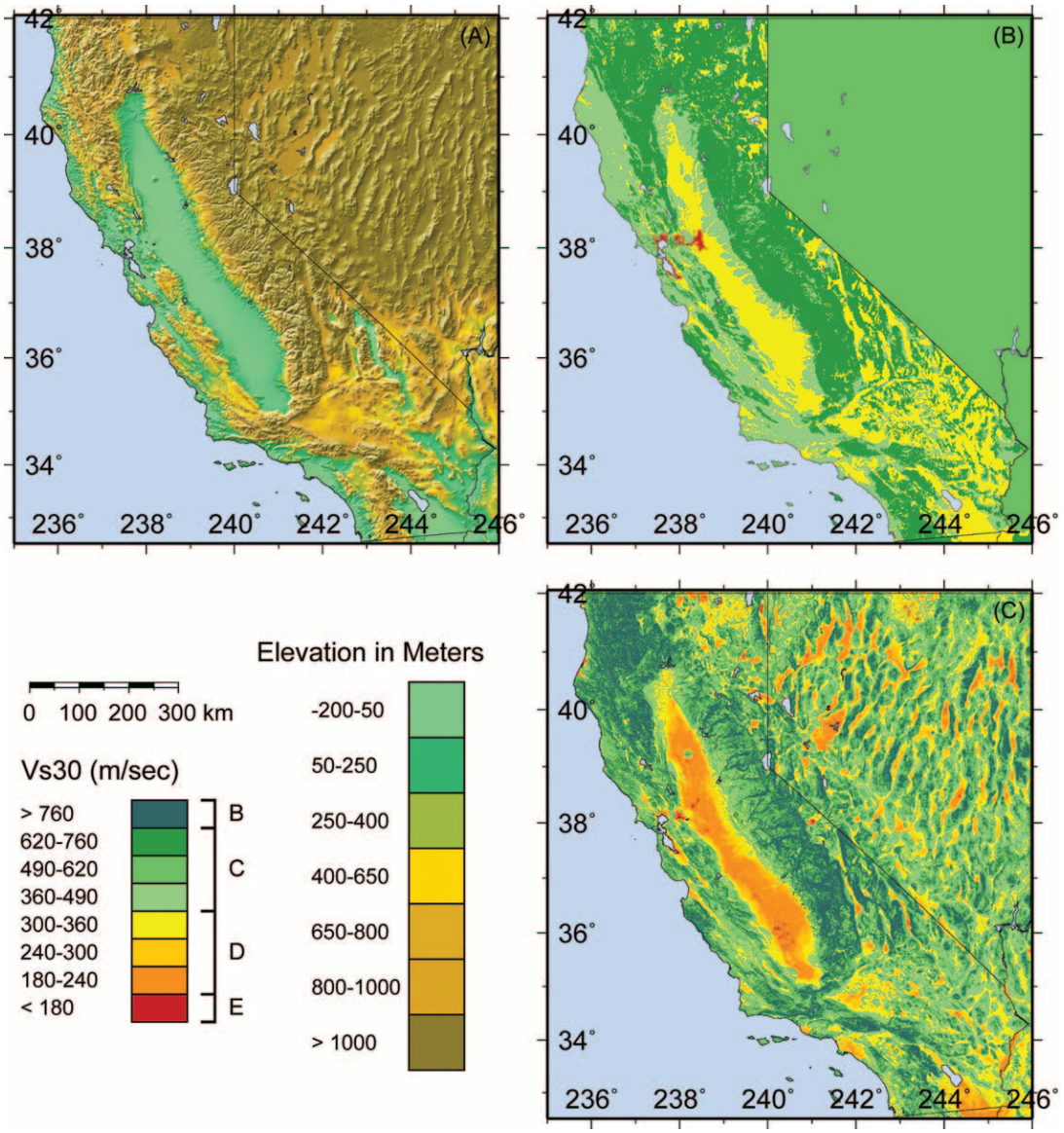

Figure 1. (a) The topographic relief for the state of California with elevation in meters (see legend). (b) Site-condition map for California based on geology and V_S observations (modified from Wills *et al.*, 2000). (c) Site-condition map derived from topographic slope using the correlations indicated in Table 2.

topography-based techniques to characterize thickness of sediment deposits for hydrologic and geomorphic purposes (e.g., Gallant and Dowling, 2003).

Whether topography alone can routinely distinguish between more subtle variations in surficial geology and, in particular, shallow site conditions (and thus ground-motion amplification) is the subject of this analysis. Our primary hypothesis is that the similarity of geology and the topography, or more specifically, the slope of topography may be exploited to provide a first-order assessment of site-dependent features of seismic hazard. This is particularly important in regions that do not possess quality surficial geology or regolith maps.

Slope of topography, or gradient, should be diagnostic of V_S^{30}, because more competent (high-velocity) materials are more likely to maintain a steep slope whereas deep basin sediments are deposited primarily in environments with very low gradients. Furthermore, sediment fineness, itself a proxy for lower V_S (e.g., Park and Elrick, 1998), should relate to slope. For example, steep, coarse, mountain-front alluvial fan material typically grades to finer deposits with distance from the mountain front and is deposited at decreasing slopes by less energetic fluvial and pluvial processes.

The motivation for deriving a relationship between topography and site conditions comes from a practical need to characterize approximate site amplification as part of an ef-

fort to rapidly predict ground shaking and earthquake impact globally. This is the key objective for the Prompt Assessment of Global Earthquakes for Response (PAGER) program of the U.S. Geological Survey National Earthquake Information Center (see Wald *et al.*, 2006). For PAGER, we need to compute empirically based ShakeMaps (Wald *et al.*, 1999a, 2005) in any region of the world that incorporates our best estimate of seismic site conditions. Relying on ground-motion predictions on rock sites rather than considering potential modification of shaking from regolith can result in differences in ground motion of up to 250% (see Table 1). This can be equivalent to more than a full unit in shaking intensity (Wald *et al.*, 1999b). Consequently, we require at least a first-order approximation of seismic site conditions for input into our ground-motion predictions. Beyond this specific application, we expect that such correlations may be useful for other seismological and geotechnical applications, including introducing site amplification to regional hazard and risk maps.

In our analysis, we first correlate 30 arc sec topographic data and V_S^{30} measurements in areas of active tectonics. We then produce V_S^{30} maps, effectively forward predictions of V_S^{30} from topographic slope, in areas where the V_S^{30} data originate and compare estimated values with observations, both visually and statistically. In addition, we compare our topographically based maps with existing V_S^{30} site-condition maps currently used for ShakeMap and other applications that are based primarily on geological maps. These analyses are then repeated for V_s^{30} data aggregated in stable continental regions. Finally, we use these correlations to produce regional-scale site-condition maps for the continental United States.

Data

Measured V_S^{30} data have been compiled from several sources. We note that V_S^{30} "data" themselves require significant interpretation and all approaches for resolving V_S^{30} are not equal, nor do they produce equivalent results. We do not appraise the quality of the V_S^{30} measurements herein. However, in our analyses, we do have the opportunity to compare the various data sets with one another within the framework of an independent parameter, namely, slope of topography.

In California, we use some 767 shear-velocity measurements (provided by C. Wills, written comm., 2005). Many of these data were used to develop the current California Site Conditions Map (Wills *et al.*, 2000). Values of V_S^{30} for Salt Lake City and the Utah ShakeMap V_S^{30} site-condition map were provided by K. Pankow (University of Utah, written comm., 2006) and represent 204 measurements gathered by the Utah Geological Survey from other sources (Ashland and McDonald, 2003). Central U.S. V_S^{30} data (432 sites in total) are obtained from R. Street (written comm., 2005). Many of these data were assembled by the work of Street *et al.* (2001) and include sites in Tennessee, Missouri, Kentucky, and Arkansas. We also acquired V_S^{30} maps used for ShakeMap purposes from network operators in California, Utah, and Memphis.

Table 1
Short-Period (0.1 to 0.5 sec) Site-Amplification Factors from Equation (7a), Mid-Period (0.4 to 2.0 sec) from Equation (7b) of Borcherdt (1994)

Class*		Short-Period (PGA)				Mid-Period (PGV)			
PGA†	V_S	<150	150	250	350	<150	150	250	350
B	686	1.00	1.00	1.00	1.00	1.00	1.00	1.00	1.00
C	464	1.15	1.10	1.04	0.98	1.29	1.26	1.23	1.19
D	301	1.33	1.23	1.09	0.96	1.71	1.64	1.55	1.45
E	163	1.65	1.43	1.15	0.93	2.55	2.37	2.14	1.91

*Class is NEHRP letter classification; V_S is mean V_S^{30} velocity (m/sec) from Wills *et al.* (2000).

†PGA is the cutoff input peak acceleration in cm/sec^2 (see Borcherdt, 1994, for more details).

Outside the United States, we use observations from Taiwan (387 sites) and Italy (43 sites) compiled by the Pacific Earthquake Engineering Research Center (PEER) Next Generation Attenuation (NGA) Project courtesy of W. Silva (Pacific Engineering & Analysis, written comm., 2006), and online at http://peer.berkeley.edu/nga/. Data for 88 sites across Australia were provided by Geoscience Australia, collected under the auspices of their National Risk Assessments Program for urban areas (e.g., Dhu and Jones, 2002; Jones *et al.*, 2005). Additional Australian data were obtained from recent spectral-analysis-of-surface-waves (SASW) surveys (Collins *et al.*, 2006) at several ground-motion recording sites. We also obtained the Taiwan national site class map for comparative purposes (C.-T. Lee, National Central University, Taiwan, personal comm., 2007).

For topography, we employ the SRTM30 30-sec global topographic data set (Farr and Kobrick, 2000). The SRTM30 data are considered an upgrade to the commonly used USGS 30-sec topographic data (GTOPO30). We use the 30-sec data in our analysis rather than some of the higher-resolution data sets available because those data are not available or complete on a global scale. Wald *et al.* (2006) showed that higher-resolution details of site conditions can indeed be recovered with 9-sec data in California, but that finer resolution is not yet uniformly available globally. Note that different resolution topographic data will result in varying slope values and may require refined correlations with V_S^{30}.

Methodology

We first correlate V_S^{30} (m/sec) with topographic slope (m/m) at each V_S^{30} measurement point for data in active tectonic areas (Fig. 2a). Color-coded symbols represent data from different geographic regions: California, Taiwan, Italy, and Utah. Figure 2b represents the correlation between V_S^{30} and the slope for stable continental regions employing measurements from Memphis and Australia. The overall trend in both figures illustrates increasing V_S^{30} with increasing

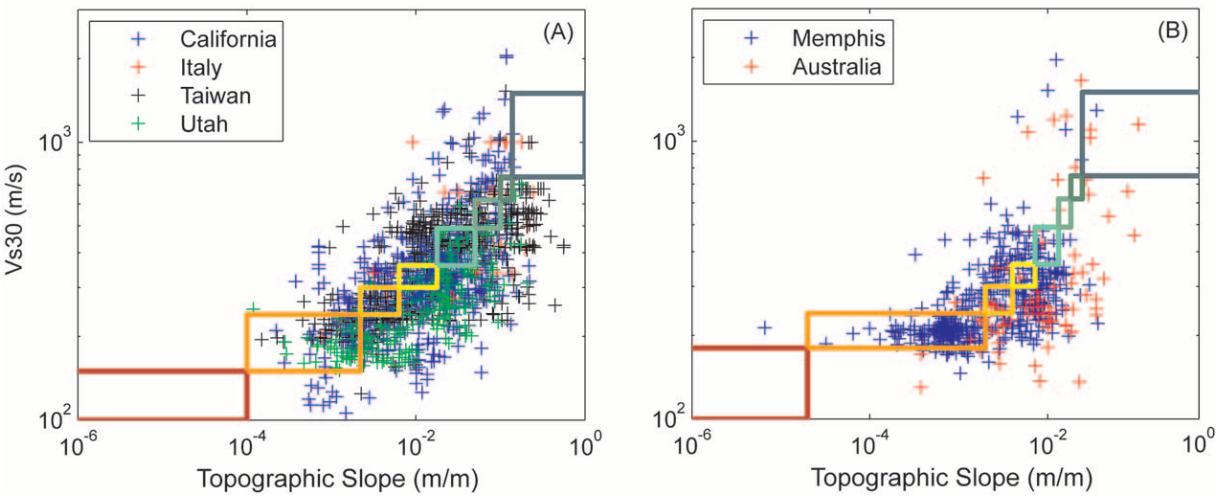

Figure 2. Correlations of measured V_S^{30} (m/sec) versus topographic slope (m/m) for active tectonic (a) and (b) stable continental regions (b). Color-coded polygons represent V_S^{30} and slope ranges consistent with ranges given in Table 2 and also consistent with the V_S^{30} legends for all geologically and topographically based maps throughout this article.

slope, indicative of faster, more competent materials holding steeper slopes. There is significant scatter, yet we will show that the trend is sufficient to be used as a reliable predictor of V_S^{30}. However, there are likely biases in data sampling; in particular, the lack of V_S^{30} measurements at steeper gradients. Most of the V_S^{30} data are found to sample relatively low gradients of less than about 7% (percent grade is the vertical rise over horizontal distance traversed), or a slope of about 4 degrees. In general, V_S^{30} measurements are collected in an effort to characterize amplification at low V_S^{30} sites rather than hard-rock sites, and those data from rock V_S^{30} sites tend to show more scatter (e.g., Wills and Clahan, 2006).

One would not expect a direct, physical relationship between slope and V_S^{30}, and in fact, no simple analytic formula emerges from the data. Curve fitting to these data requires subjective weighting, coupled with assignment of initial and ending values where there are fewer data to constrain the relations. Rather, we chose to characterize the relationship in terms of discrete steps in shear velocity values tied to National Earthquake Hazards Reduction Program (NEHRP) V_S^{30} boundaries (Federal Emergency Management Agency [FEMA] 222A, 1994). The NEHRP boundaries are further subdivided into narrower velocity windows to increase resolution where possible. Topographic slope at any site that falls within these windows is assigned a V_S^{30} that defines the median value of the subdivided NEHRP boundaries (Fig. 2; Table 2). Note that we did not use the Utah V_S^{30} data in developing these correlations. It is observed that these data possess systematically low shear velocity for a given slope from mean values of the other regions. We discuss the implications of this omission later.

We have also performed multiple linear regression analyses on both slope and elevation, attempting to correlate them jointly with V_S^{30}. Essentially, slope and elevation themselves correlate well, but elevation alone is, in general, a poorer predictor of V_S^{30} than slope. There are many areas of low slope over a wide range of possible elevations, so joint analysis proved weaker than using slope alone.

Application in Active Tectonic Regions

California

We compute V_S^{30} for all of California, applying the topographic slope ranges shown in Table 2 (for active tectonic regions) to produce the map shown in Figure 1c. A direct comparison with the topographic V_S^{30} predictions can be made from the California statewide map of surface geology (Fig. 1b; modified from Wills *et al.*, 2000). One significant difference between the slope-derived map of V_S^{30} (Fig. 1c) and the geology-based Wills *et al.* (2000) map (Fig. 1b) is that the former allows more continuous variations in V_S^{30}, but the latter assigns V_S^{30} values to all occurrences of that geological unit to a constant (mean V_S^{30}) value. Consequently, the relatively few colors for the Wills *et al.* (2000) map are a consequence of the few discrete geological units that were classified. Wills and Clahan (2006) present further subdivisions based on geological considerations that may provide a more precise assignment of V_S^{30} variations.

To provide more rigorous validation for this technique, we present histograms that indicate the (log) ratio of measured V_S^{30} values and those estimated from topographic slope for the same sites in California (Fig. 3a). Figure 3b shows the equivalent plot when we compare measured V_S^{30} with those velocities assigned by Wills *et al.* (2000). Neither comparison has a significant bias, and the slope-determined and geologically based values have comparable scatter.

Table 2
Summary of Slope Ranges for NEHRP V_S^{30} Categories

Class	V_S^{30} Range (m/sec)	Slope Range (m/m)	
		Active Tectonic	Stable Continent
E	<180	<1.0E−4	<2.0E−5
	180–240	1.0E−4–2.2E−3	2.0E−5–2.0E−3
D	240–300	2.2E−3–6.3E−3	2.0E−3–4.0E−3
	300–360	6.3E−3–0.018	4.0E−3–7.2E−3
	360–490	0.018–0.050	7.2E−3–0.013
C	490–620	0.050–0.10	0.013–0.018
	620–760	0.10–0.138	0.018–0.025
B	>760	>0.138	>0.025

To examine the topographic approach in more detail, Figures 4 and 5 indicate more detailed maps centered on the high-seismic-risk areas of the San Francisco Bay area and the Los Angeles region, respectively. Owing to the investment of intensive geophysical and geotechnical investigations, significant portions of our V_S^{30} data are obtained from these heavily populated regions. Direct comparison of the measured V_S^{30} values (colored circles) on Figures 4a and 5a with the Wills *et al.* (2000) map (Figs. 4b and 5b) and with corresponding slope-derived values (Figs. 4c and 5c) proves informative. There is a favorable agreement between the Wills *et al.* (2000) V_S^{30} map and the slope-derived V_S^{30} maps. However, the slope-derived maps predict wider ranges in V_S^{30} that appear more spatially variable than the geology-based maps. Conversely, geology-based values are typically taken as constants within a specific geological unit, independent of any slope variations that may correlate with changing material properties (mostly particle size) and thus with V_S^{30} values.

Even at this scale, in the San Francisco Bay Area many of the details of the geology-based (4b) and topography-based (4c) maps are recovered, and the automated assignment of near sea level elevations to near the DE boundary seems to mimic the mapped extent of this site class. Correspondence between classes C near the BC boundary are less well recovered, but fortunately the overall error in site amplification introduced by misclassifying C for BC, or vice versa, is then about 10% (see Table 1). Similar correlation is seen in the maps for the Los Angeles region (Fig. 5). Here, additional areas near the DE boundary are present in the slope map (Fig. 5c) that are not seen on the geology map (Fig. 5b). The abundance of surficial material near the DE boundary on the topographically based map appears consistent with the measured data that are superimposed on the topographic map (Fig. 5a). However, corresponding higher-velocity areas on the geologically based map could be classified near the DE boundary based on both borderline low V_S^{30} (for class D) observations and small particle sizes (C. Wills, California Geological Survey, personal comm., 2005).

Note that the resolution (30 arc sec) of the topography allows for detailed maps of site conditions. Many of these details come from small-scale topographic features that are likely to be manifestations of real site differences, such as basin edges and hills protruding into basins and valleys and are thus easily visible due to their significant slope change signatures. Typically, these edges are important for predicting ground-motion variations due to earthquakes. Again, higher-resolution topography is available for this area of the world so additional details could be resolved.

Taiwan

The next question we address is whether the correlations hold in areas of similar overall topographic expression but which exhibit radically different geology, tectonics, and geomorphology. Taiwan was chosen to test this hypothesis, primarily because the site classes on a national scale are well understood (Lee *et al.*, 2001) and are available for direct comparison. The abundance of V_S observations used in our correlations provides us with a valuable validation case study to ensure that the slope calibration with V_S^{30} is robust among our base data set. Figure 6a indicates the topographic map superimposed with color-coded V_S^{30} measurements, the national site classification map (Fig. 6b; modified from Lee *et al.*, 2001), and the topographic-gradient-derived V_S^{30} map for the island of Taiwan (Fig. 6c). V_S^{30} values around Taiwan vary widely, but they do so with rather systematic trends that are well recovered using topographic slope.

Figure 3c provides an overview of the ratio of measured versus slope-derived V_S^{30} values. The mean and standard deviation are comparable to those evaluated for California sites. In presenting the Taiwanese site class map, we have assigned median shear-wave velocities based on the NEHRP categories adopted by Lee *et al.* (2001). The exception for this being site class E, where we assigned a V_S^{30} of 150 m/sec. The topographically derived site class map for Taiwan appears to provide a slightly better fit to V_S^{30} observations (Fig. 3c) than the geologically based map (Fig. 3d). However, there may be some bias in our statistical comparisons owing to our assignment of V_S^{30}. The Taiwanese are currently working on a revised site-classification scheme that should further improve comparisons with observed data

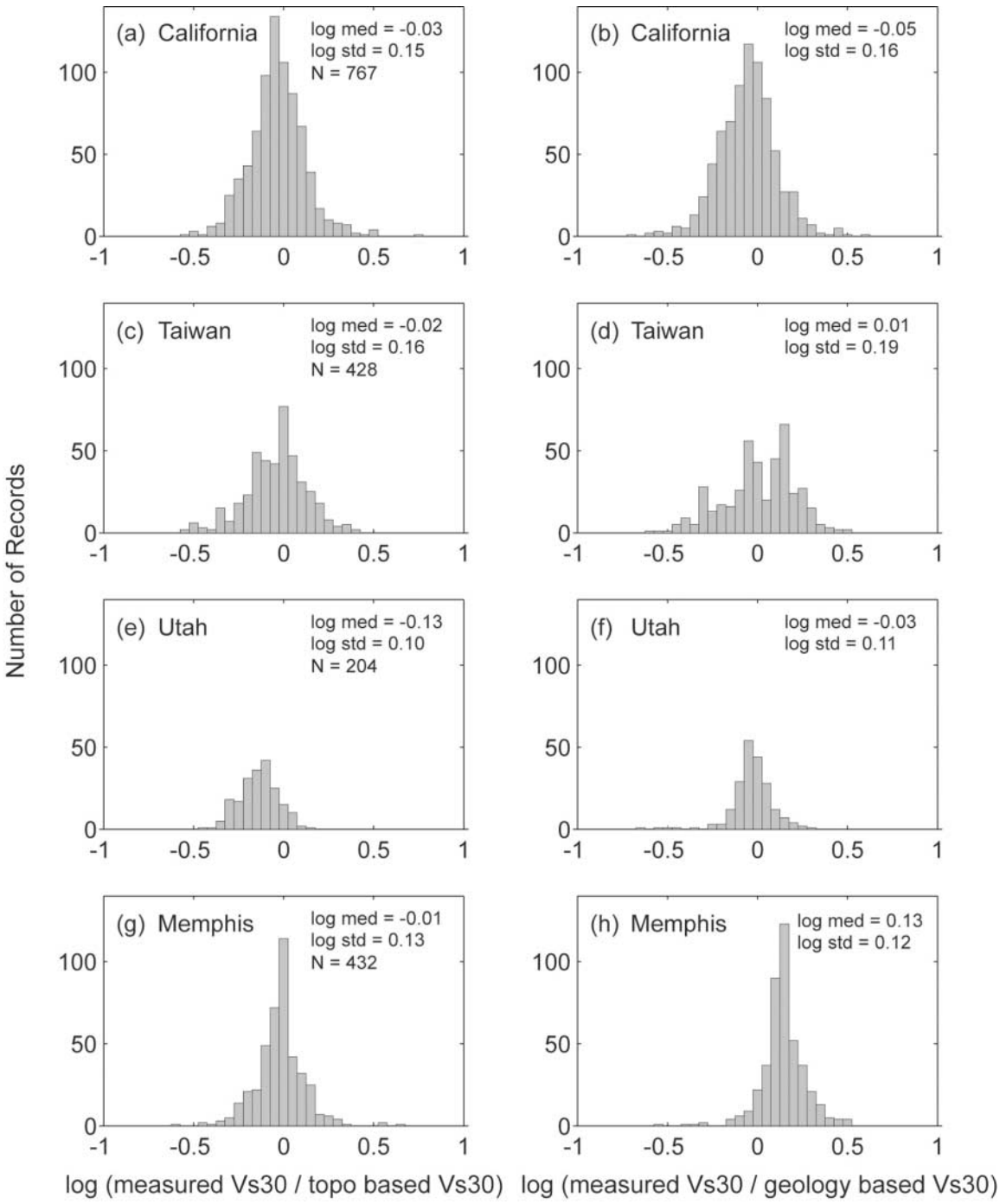

Figure 3. Histograms indicating logarithmic differences of measured V_S^{30} values compared with values derived from topographic slope correlations (a, c, e, and g) or based on existing V_S^{30} site-condition maps (b, d, f, and h). N is the number of V_S^{30} measurements.

(C.-T. Lee, National Central University, Taiwan, written comm., 2007).

Note that in a significant number of the examples represented in this report that population exposure tends to correlate very well with slower V_S^{30} site conditions as calculated from the slope of topography. Intuitively this is not surprising because steep hill slopes are not usually as desirable for building structures, whereas flat-to-gently sloping lands tend to consist of more fertile soils suitable for agricultural purposes and have traditionally been inhabited. Using Taiwan as an example, we compare seismic site condition with population exposure as derived from the Oak Ridge National Lab-

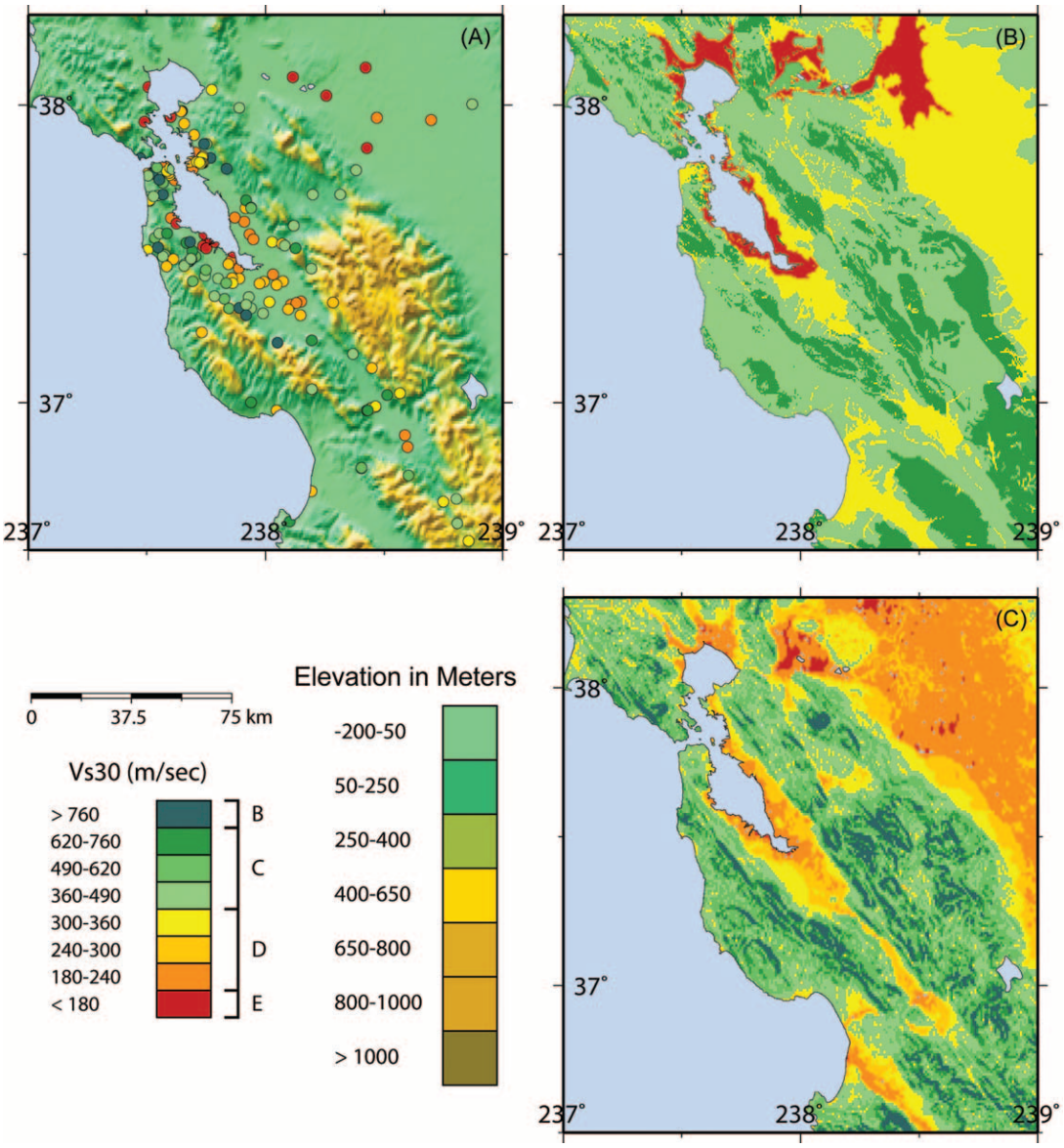

Figure 4. (a) Topographic map of the San Francisco Bay Area. Circles indicate the location of measurements, color-coded by V_S^{30} in meters per second (see left-hand legend). (b) Site-condition map based on geology and V_S observations (modified from Wills *et al.*, 2000). (c) Site-condition map derived from topographic slope.

oratory's LandScan 2005 database (e.g., Dobson *et al.*, 2000; Bhaduri *et al.*, 2002) (Fig. 6d). We see that urban communities appear to be most dense in the flat-lying lands that correspond to lower V_S^{30}. In particular, the region around Taipei possesses significant amplification potential owing to is location on primarily NEHRP site class D surficial material. Population density becomes less dense as we grade from gently sloping to steeper terrains. This figure serves to remind urban planners, disaster mitigators, and emergency responders why we must consider seismic site conditions as an important component in earthquake hazard assessment, because those areas with the densest populations are also likely to have strong site amplifications.

Salt Lake City

The final example of active tectonic regions is that of the Salt Lake City, Wasatch Front region. This can be considered a forward prediction, because, unlike California and Taiwan, no V_S^{30} data for this region were used in our calibration analysis. The data, which were obtained from the Utah Geological Survey, appeared to have V_S^{30} values systematically lower than mean values from other active regions with similar slope (Fig. 2a). The geologically and topographic slope-based maps (Fig. 7b and c, respectively) demonstrate similar trends. However, there appears to be a significant shift toward lower velocities in the geologically

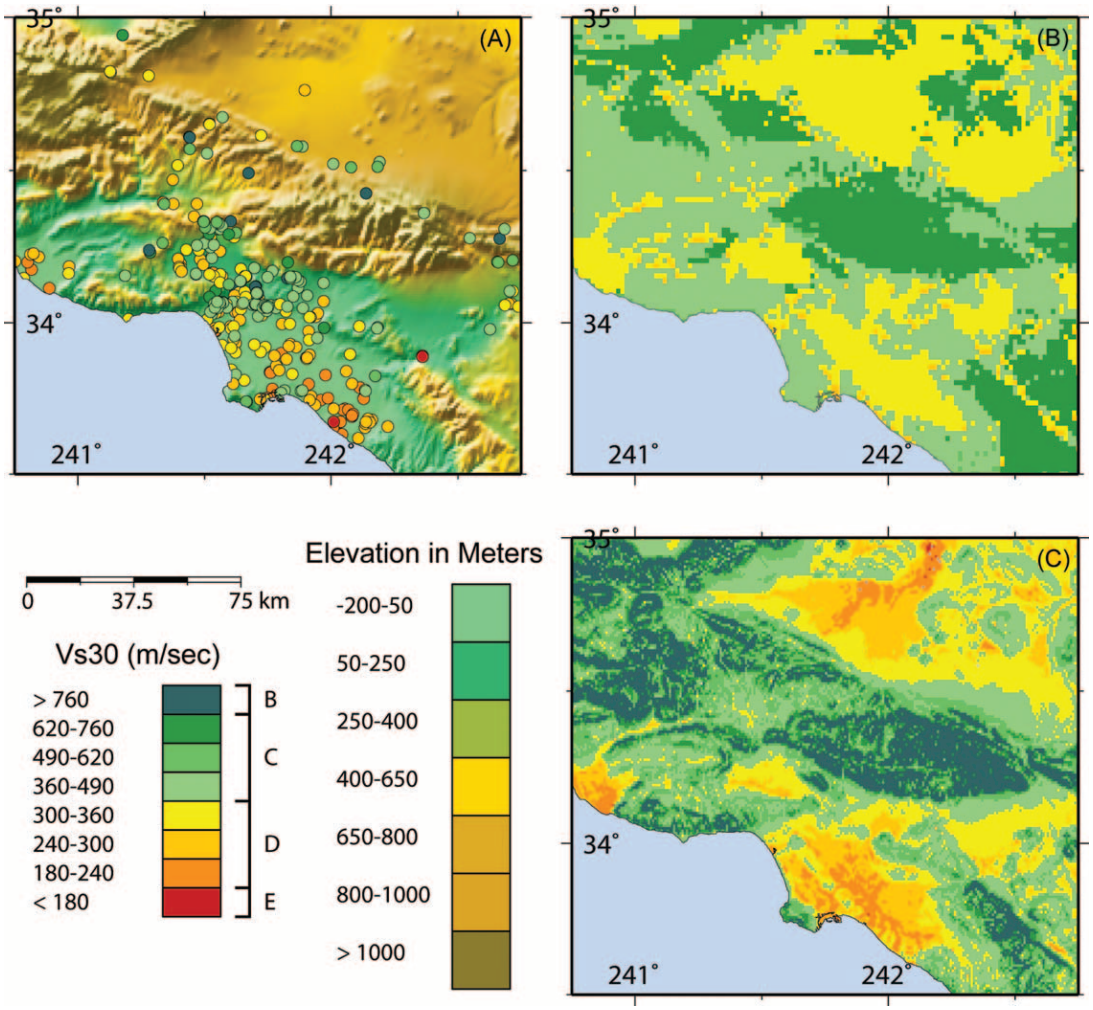

Figure 5. (a) Topographic map of the Los Angeles region. Circles indicate the location of measurements, color-coded by V_S^{30} in meters per second. (b) Site-condition map based on geology and V_S observations (modified from Wills *et al.*, 2000). (c) Site-condition map derived from topographic slope.

based site map, consistent with the measured data. On average, the geology-based map (Fig. 3f) represents the measured data better than the slope-derived map (Fig. 3e). The latter shows a slight overall bias indicating that V_S^{30} in the Salt Lake City region are on average overpredicted by the topographic-slope approach employing the current correlations. It is possible that near-surface shear-wave velocities in the region are lower for a given slope angle than in California and Taiwan and thus require slight modification to the slope versus V_S^{30} correlation. Alternatively, the V_S^{30} measurements underestimate actual *in situ* velocities for some other reason, not yet established. Although we observe that the slope-derived map (Fig. 7c) indicates a more natural progression of V_S^{30} grading higher values toward steeper topography, it is also possible that Lake Bonneville deposits that abut the mountain front, rather than sloping (K. Pankow, University of Utah, personal comm., 2007), may violate the basic assumption under which our correlations are based. The small overall bias in the Salt Lake City region could be removed with a overall shift of about 25% in predicted V_S^{30} values, though it is likely that these biases are dominated in particular geological units.

Application in Stable Continental Regions

Memphis, Tennessee

As expected from basic geomorphology, in areas of significant relief, mountains correlate well with rock and basins correlate well with sediments. Will this approach work in areas of lower overall relief? Although a similar range of V_S measurements, from hard rock to soft sediments, exists in the Mississippi Embayment, the associated topography is much more subdued, as indicated by the narrow range in elevation (Fig. 8a). Hence, there is less variation in slope, and consequently, it might be expected that it would be more

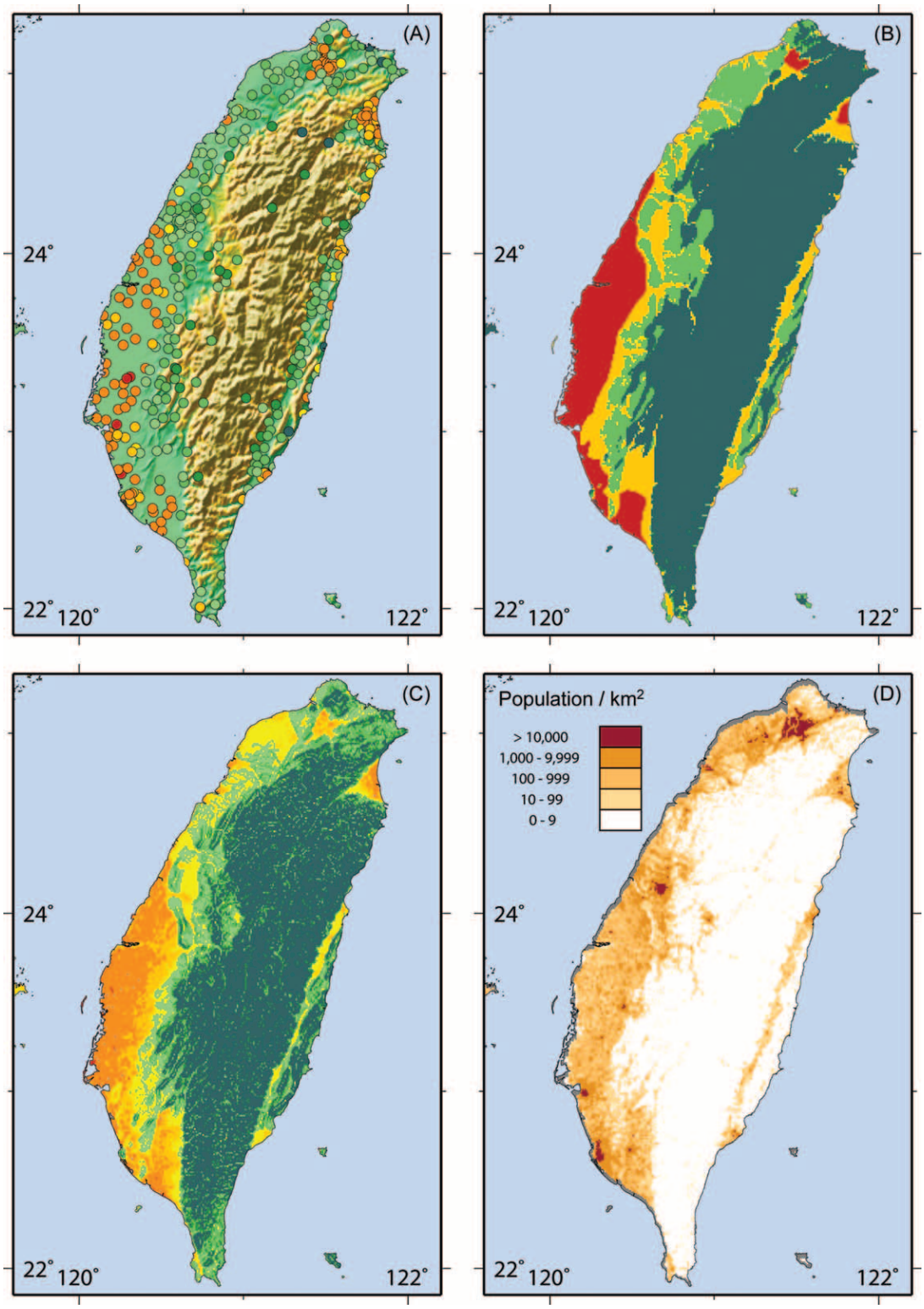

Figure 6. (a) Topographic map of Taiwan with elevation in meters. Circles indicate the location of measurements, color-coded by V_S^{30} in meters per second. (b) Site-condition map based on geology and V_S observations (modified from Lee *et al.*, 2001). (c) Site-condition map derived from topographic slope. (d) Population density map of Taiwan derived from the LandScan 2005 population database (e.g., Dobson *et al.*, 2000; Bhaduri *et al.*, 2002). See Figure 1 for topography and V_S^{30} legends.

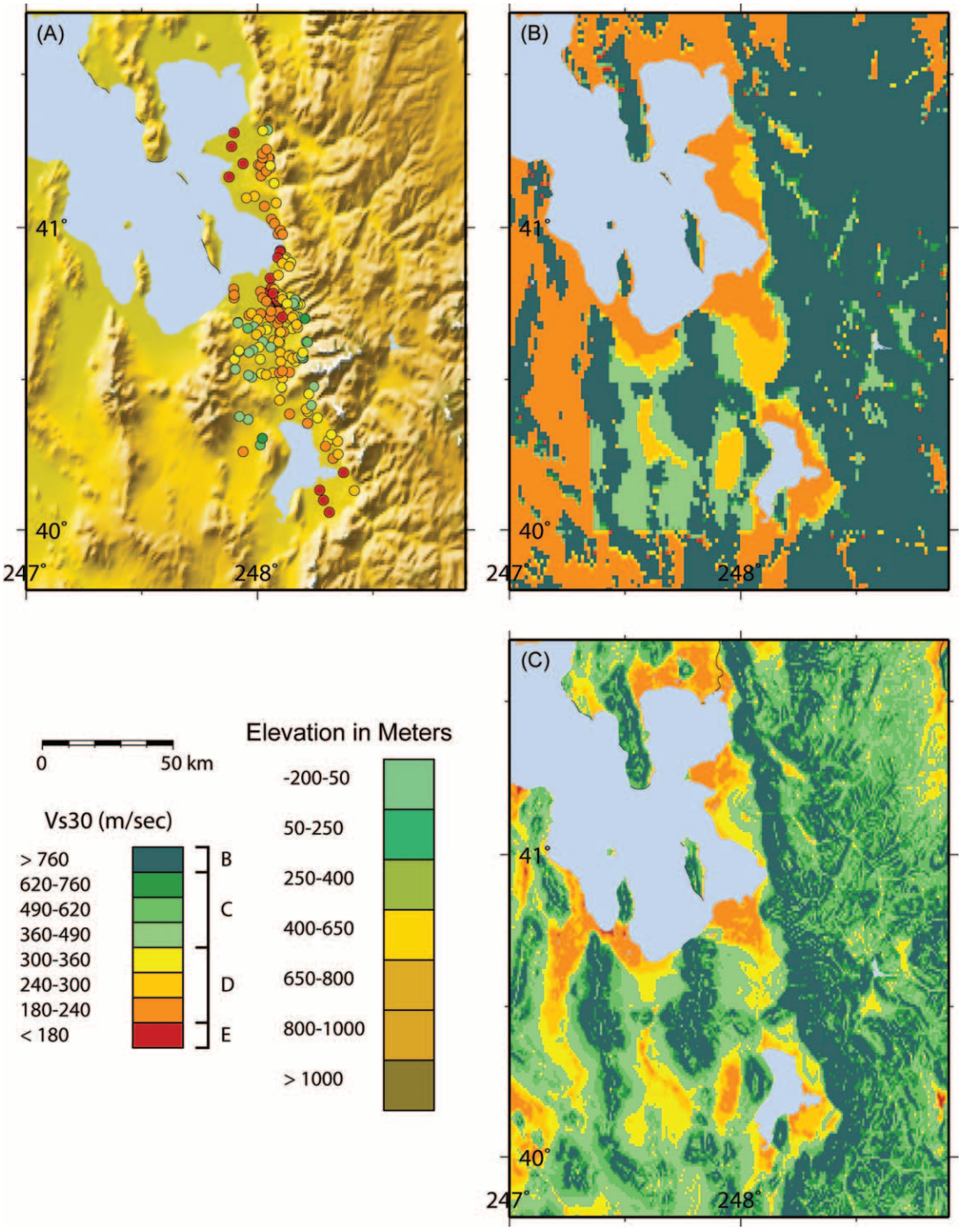

Figure 7. (a) Topographic map of the Salt Lake City, Wasatch Front region of Utah. Circles indicate the location of measurements, color-coded by V_S^{30} in meters per second. (b) Site-conditions map based on geology and V_S observations. (c) Site-condition map derived from topographic slope.

difficult to assign slope ranges that define the V_S^{30} categories. Furthermore, as in the active tectonic regions, few V_S^{30} measurements are available for high-velocity, hard-rock sites. Nonetheless, there does appear to be a natural progression among V_S^{30} values plotted against slope for both the central United States and Australia (Fig. 2b) and we use these limits to produce the slope-based site-condition map for the Mississippi Embayment region shown in Figure 8. We compare the 432 V_S^{30} measurements with topography (Fig. 8a), the V_S^{30} site-condition map (Fig. 8b) used for the regional

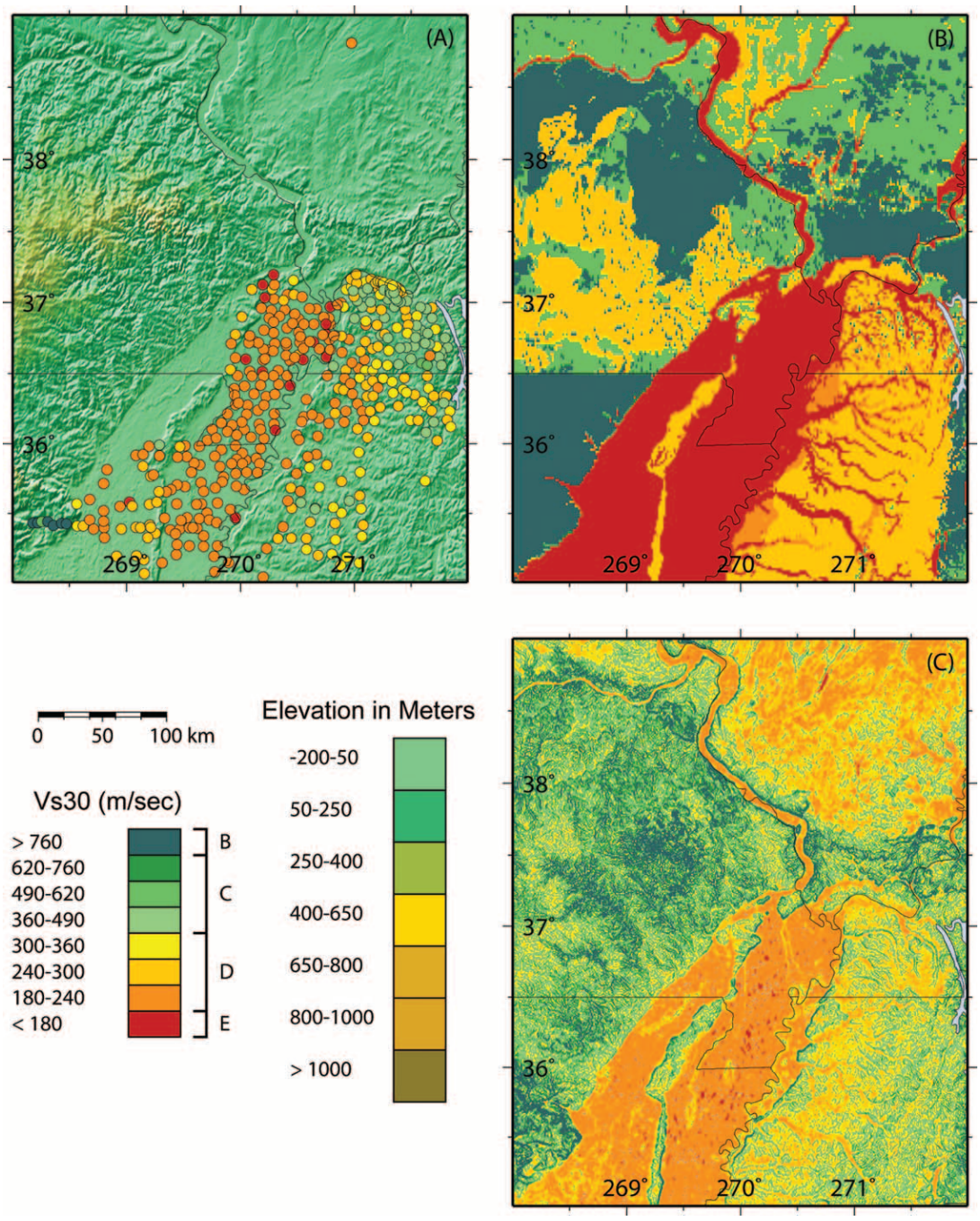

Figure 8. (a) Topographic map centered on Memphis, Tennessee, showing the Mississippi Embayment region of the central United States. Circles indicate the location of measurements, color-coded by V_S^{30} in meters per second. (b) Site-condition map based on geology and V_S observations (modified from Brackman, 2005). (c) Site-condition map derived from topographic slope.

ShakeMap installation (Brackman, 2005), and the slope-derived V_S^{30} map (Fig. 8c) at sites in the Mississippi Embayment.

We find excellent correspondence of measured and slope-estimated V_S^{30} values. Both the lowest V_S^{30} regions, in particular those along river channels and in the Mississippi Embayment itself, are recovered, as are the few relatively high-velocity V_S^{30} values in the southwestern corner of the map. On average there is very little bias to the estimates (Fig. 3g). The same cannot be said of the geology-based site-condition map (Fig. 8b), which shows an overall bias, having significantly lower V_S^{30} values with respect to those mea-

sured (Fig. 3h). Likewise, there is a more natural progression of varying V_S^{30} in the topography-based site map (Fig. 8c) than in the geology-based map (Fig. 8b). Furthermore, the current map shown in Figure 8b, used by the Central United States Earthquake Consortium (CUSEC), itself shows significant inconsistencies across state borders because they were mapped independently by different researchers.

Consequently, it appears that the slope versus V_S^{30} categories for this region of low topographic relief can be used successfully as a proxy for basic site conditions as it does for tectonically active regions. Another redeeming feature is that either the slope range or mean slope values for a given region can provide simple quantitative diagnostics for the nature of the topographic relief in a given area from which appropriate V_S^{30} versus slope range assignments can be obtained. For example, mean slope values for the active tectonic regions are about 0.07; for the Mississippi Embayment the mean slope is much lower, at 0.01, and over the entire continental United States east of the Rocky Mountains, the slope mean is about 0.04. Hence, we can use the mean slope to establish which slope correlations should be employed: active tectonic or stable continent. Alternatively, simplified characterizations of tectonically active versus stable continent domains could suffice in choosing between the coefficients employed for slope-based V_S^{30} assignments.

Application for the Continental United States

Equipped with these correlations between topographic slope and V_S^{30}, and assuming either stable continent or tectonic coefficients for slope versus V_S^{30} apply, we can readily generate maps of estimated V_S^{30} velocities for any region around the globe. As an example, we describe regional evaluation of site classes for the continental United States in the following sections.

Western United States

We apply the slope and V_S^{30} relations developed for active tectonic regions for the western margin of continental United States, west of the Front Range of the Rocky Mountains (Fig. 9). The regional topographically based site class map indicates broad regions of contrasting site conditions throughout the western United States, with faster material associated with much of the Rocky and Cascade Mountain ranges and slower material interspersed in the lower-lying basins. In Nevada, in particular, we observe highly variable, and periodic, changes in site class associated with the Basin and Range (also see Fig. 1c). It is also noteworthy that this map has excellent correspondence with the U.S. national surficial materials map (Soller and Reheis, 2004). We observe that regions of different surficial material tend to produce different site class signatures. Lacustrine sediments that cover much of western Utah are also well recovered.

As noted in northeast California (Fig. 1), regions of recent volcanism are interpreted as having relatively slow velocities on our topographically based site class map. This is because the associated lava flows have relatively low topographic gradient. In addition to areas of northern California, this is particularly apparent in southern Idaho and central Oregon, east of the Cascades. This observation highlights one of the limitations in using this technique in broad-scale applications. One must be aware of existing geological conditions within the region of interest that may affect the reliability of this approach.

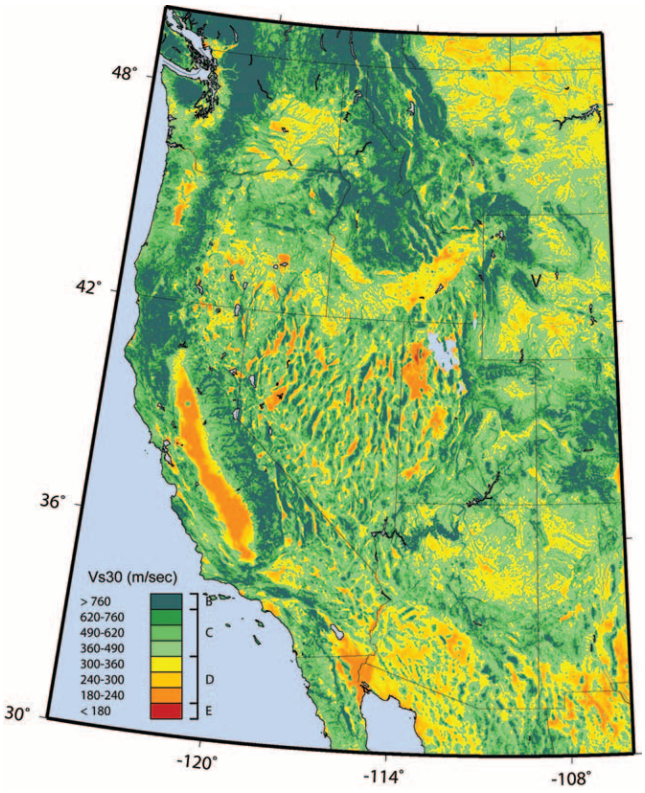

Figure 9. Estimated site-condition map for the continental United States west of and including the Rocky Mountains, derived from topographic slope and slope-V_S^{30} correlations for active tectonic regions (see Table 2).

Eastern United States

We also apply our approach using the stable-continent slope-V_S^{30} correlations to produce a V_S^{30} map of the entire continental United States, east of the Rocky Mountains in Figure 10. Again, the seismic site-condition map produced recovers many of the surficial features described by Soller and Reheis (2004). In particular, the Appalachians indicate relatively fast-velocity material, consistent with their steeper terrain and relatively high topographic relief. The Atlantic and Gulf coasts indicate slower material, corresponding to coastal zone sediments. Glacial deposits adjacent to the Great Lakes region are also well recovered (Soller and Reheis, 2004). Our topographic slope correlations likely underpredict V_S^{30} in areas where flat-lying carbonate rocks

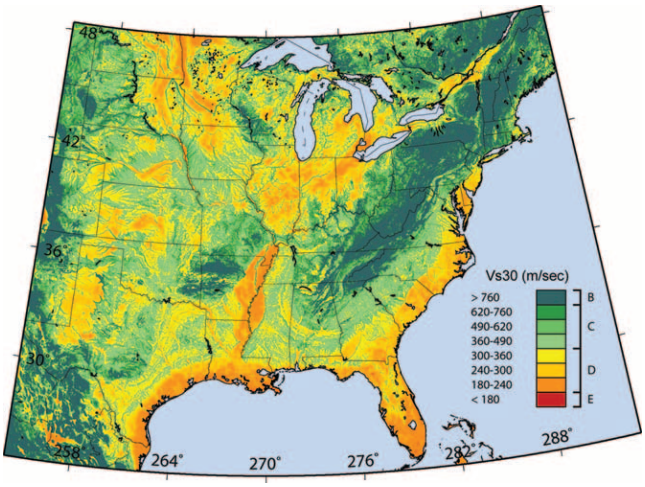

Figure 10. Estimated site-condition map for the continental United States east of the Rocky Mountains, derived from topographic slope and slope-V_S^{30} correlations for stable continent (see Table 2).

dominate (for example, southern Florida), but the lack of V_S^{30} measurements or site-condition maps precludes direct comparison. These carbonates may have varying degrees of weathering and surficial deposits that preclude regional, broad-brush V_S^{30} classification (e.g., A. McPherson and L. Hall, unpublished manuscript, 2007). Note that had southern Florida ranked high for earthquake hazards, such information would likely be more readily available; its low hazard warrants a more regional approach at this time.

Although some aspects of these maps may be approximate, they do provide first-order V_S^{30} site-condition maps for the continental United States, with very little effort. One obvious side benefit of this approach is that this map requires only our correlation, a digital 30-sec topographic map, and a few seconds of computer time to produce. Maps and grids of estimated V_S^{30} based on topographic slope for many seismically active areas of the world are presented in T. Allen and D. J. Wald (unpublished manuscript, 2007).

Discussion

Why would topographic slope provide such a good proxy for the average V_S in the top 30 m? A discussion of wide range of geological materials and erosional and depositional domains, and their influence on the physical properties controlling V_S is beyond the scope of this discussion. However, some limited examples of widespread geomorphic domains are warranted. We consider the physical properties that most influence shallow V_S in soil and rock separately.

Why Topographic Slope Works as a Proxy for V_S^{30}

Of the physical properties of soils, those that have a strong affect on shear modulus are most pertinent to V_S. In general, void space and effective mean stress dominate shear modulus changes, because density variations tend to be rather small in soils (Fumal and Tinsley, 1985). When considering only shallow (top 30 m) conditions, mean principal effective stresses do not vary dramatically. Hence, among physical parameters, void ratios are one of the most important factors affecting shear modulus. Fumal and Tinsley (1985) find that the soil texture and the relative grain-size distribution can be a good measure of void ratio. For the San Francisco Bay Area, they divided the soils into four textural categories based on grain-size distribution and found that, in general, shear-velocity increases as mean grain size increases. That V_S increases with increasing grain size goes a long way to explain why lower V_S and lower topographic slope correlate so well; particle size decreases as the available energy in the depositional environment decreases (with lower slopes).

In rock, Fumal and Tinsley (1985) show that the two dominant physical properties determining V_S are hardness and fracture spacing, with greater hardness and spacing resulting in higher velocities. Here too, we would expect that these parameters would correlate with topographic slope because hard rock and coarse fracture spacing both resist weathering, allowing rocks with higher V_S to hold a steeper slope.

In typical semiarid alluvial fan systems, such as much of the western United States, mountain fronts grade from bedrock to steep, deep channels, grading midfan to shallower, braided channels, to the outer fan, where channels are very shallow and braided (e.g., Blatt *et al.*, 1980). In general, there is a decrease in grain size down fan as the importance of stream-flow deposits dominates that of debris-flow deposition. With increasing distance from the mountain front, floodplain deposits continue to decrease in particle size as deposited at decreasing slopes by less energetic fluvial and pluvial processes.

Naturally, our preceding generalization applies only to the overall trend of fining particle size with lower gradients, and hence lower V_S^{30} with lower slope within a particular depositional setting. There are also several reasons why topographic slope should be limited in its ability to recover V_S^{30} by several known geological processes and overall variations in geological materials. Clearly, other processes can modify or control particle size and other factors that determine V_S^{30} in any depositional environment, such as variable source material, sorting, cementing, channeling, etc. These will presumably lead to substantial variation on the overall trend we observe. For example, in many western U.S. soils, the age of the soil development and weathering will influence V_S^{30}, with perhaps little change in topographic slope. Soil aging, in particular calcite cementation of soils (a.k.a. caliche) in the Las Vegas Basin, Nevada, has been shown to elevate V_S^{30} values to 500–600 m/sec (Scott *et al.*, 2006), despite relatively low slopes. Fortunately, such rigid soil should be expected to hold considerable slope under erosional (stream-cutting) influences, so the overall trend may still be consistent with our simple assumptions.

Thelen *et al.* (2006), based on V_S^{30} profiles in the Los Angeles Basin, suggest that slope also controls the distribution of clay minerals in the basin, which they describe as key in the designation of mappable soil units, and that slope also controls texture, which in turn affects the porosity of the type of soil formed. Thelen *et al.* (2006) further conclude that the best surface indicator of V_S^{30} may be the hydraulic gradient of the San Gabriel River, another manifestation of the influence of slope. Yet, they rightly caution that only to the extent that soils are predictors of hydraulic gradient, may they also be considered only rough predictors of V_S^{30}.

Our simple assumption on the correlation of slope and V_S^{30} will break down for some obvious topographic and geomorphic combinations. For example, in continental glaciated terrains, topography alone cannot distinguish between topographically similar depositional (glacial till) drumlins and erosional (bedrock) roche moutonnées. Likewise, and more extensive in area, nominally flat volcanic plateaus may not be recognized as rock because they can have low overall slope. The latter case happens to be quite common for much of northeastern California, where significant areas of hard rock (Fig. 1c) are assigned to soft rock or soil based on our procedure due to regions of low slope (Fig. 1a). Because our goal is to quantify shaking in populated areas, and unweathered volcanic plateaus tend to be sparsely populated, in particular compared with the many urbanized low-sloping alluvial basins, this misclassification may not lead to significant uncertainties in loss or damage assessments.

Alternatively, it is likely that other readily available characteristics of topography may further elucidate the difference, even between low gradient soils and rocks. For example, spatial roughness determined at high resolution may allow distinguishing between smooth depositional sediments and rougher volcanic rock despite similar slopes. Additional digital geographic and/or geomorphic data may also be exploited to this end as well; in particular, land use data may distinguish between comparable slopes of varying materials in many cases. For example, Matsuoka *et al.* (2005) found a good correlation between slope, along with geomorphic indicators (for example, man-made fill versus natural fill, distance to mountain front, etc.) with V_S^{30} in Japan. However, we have purposely limited our study to easily exploited topography data; further analysis is underway to provide additional constraints on V_S^{30} in areas that may violate our simple topographic slope versus V_S^{30} assumptions.

Comparison with Geologically Based V_S^{30} Maps

We should emphasize that our direct comparison with other V_S^{30} maps derived from maps of regolith and bedrock geology does not imply that we have full confidence in the details of either. Rather, consistencies and inconsistencies become more apparent with direct side-by-side comparison. Only on very local scales with dense V_S^{30} sampling are V_S^{30} maps fully constrained, and then typically only along profiles (e.g., Thelen *et al.*, 2006; Scott *et al.*, 2006).

Because geology-based maps are typically mapped with completely different goals in mind than constraining seismic site amplification, there are some obvious drawbacks to using them as a starting point for mapping site conditions. Standard geologic maps ordinarily contain little information about the hardness or fracture spacing of bedrock units, so estimating shear velocity is difficult (Fumal and Tinsely, 1985). Because bedrock V_S^{30} values are sparse, assignments to mapped bedrock units from observational V_S^{30} measurements are often uncertain. In soils, geotechnical properties (including cone penetration test results, thickness, and grain size) beneficial for detailed V_S^{30} assignments (e.g., Holzer *et al.*, 2005) are often lacking and V_S^{30} measurement localities are often poorly dispersed.

In our analyses we have shown to some degree that geologically based V_S^{30} maps can have deficiencies with respect to predicting V_S^{30} measurements. This is in part because assignments of single V_S^{30} values to an individual geological unit does not capture the potential variability of V_S within the unit. One clear limitation is the lack of information on the depth variations of particular units; these thickness variations result in variable V_S^{30} values that are not accommodated. Furthermore, basement geology maps sometimes ignore the thin veneers of regolith that are important for constraining ground-motion amplification, where the underlying bedrock is well known. Another concern with geology-based maps is that variations in grain size within a unit (often associated with variable weathering profiles) can alter wave speeds, yet geological units are assigned single V_S^{30} values. Topographic slope, however, does correlate with grain size, so aspects of this variability are captured with our approach to mapping V_S^{30}. At the very least, slope-based V_S^{30} maps allow more continuous changes in V_S^{30} within single mapped geological units if the unit exhibits measurable variations in slope.

Most existing site-classification maps have been derived primarily from existing or reinterpreted geological maps (e.g., Fumal and Tinsley, 1985; Park and Elrick, 1998; Wills *et al.*, 2000; Wills and Clahan, 2006). Fumal and Tinsley (1985) predicted shear-wave velocities across southern California from geology based on 84 velocity borehole profiles. Their approach involved interpretation of different Quaternary alluvial units along with their lithologic characteristics. Such an approach precludes assigning V_S^{30} values without assigning such characteristics, usually from borehole logs, so substantial geotechnical information is required. Alternatively, Park and Elrick (1998) also predicted V_S^{30} values in southern California from more detailed geological maps and found that their more numerous V_S^{30} measurements (196) warranted only three age-designated subdivisions (Quaternary, Tertiary, and Mesozoic) to fully separate the measured V_S^{30} ranges.

Wills *et al.* (2000) used V_S^{30} measurements from 556 profiles in conjunction with California geological maps to produce a statewide V_S^{30} site-condition map by grouping geological units with similar physical properties into cate-

gories that were expected to have comparable V_S values. Like Park and Elrick's approach, no additional geotechnical information is required for units once their geological versus V_S^{30} correspondence is ascertained, making their approach tractable for a statewide application. The Wills *et al.* (2000) V_S^{30} maps have been widely used for hazard studies and form the basis for site corrections in ShakeMap in California (Wald *et al.*, 2005).

More recently, Wills and Clahan (2006) further distinguished between geological units by grouping geological units by age and then splitting units by texture and thickness of alluvial deposits. While this approach may reduce the number of misclassified sites, it also requires additional effort and more geotechnical information than simply sorting geological units from existing geological maps. A full map for California using this approach is under development according to Wills and Clahan (2006); a substantial effort that is certainly warranted given the earthquake hazard and risk to major urban centers in California. In comparison, our approach is readily available for our global ShakeMap efforts. We expect to supplant our topographic-based V_S^{30} maps with more detailed regional V_S^{30} maps as they are further developed.

Conclusions

We have developed a simple, inexpensive method for delivering first-order seismic site-classification maps that can be used to rapidly estimate potential ground shaking following large global earthquakes in the absence of detailed geologically based maps. This process has been developed primarily for ShakeMap and PAGER applications. However, the technique has potential to be used more widely in scenario and probabilistic earthquake hazard and risk assessments for disaster response and mitigation programs anywhere in the world.

We exploit the natural correlation between topography and surficial geology to derive topographic slope bounds that allow automatic mapping of V_S^{30} suitable on a regional scale anywhere on the globe. Because we are concerned with earthquake ground motions, and earthquakes occur predominantly in regions with significant tectonic relief, the V_S^{30} versus topographic slope correlation for tectonic regions (dominated by data from California and Taiwan) should hold under most circumstances. In stable continental areas that tend to exhibit more subdued topography (like the central United States), V_S^{30} values can also be recovered, but the correlation with slope is modified to accommodate the general observation that rock sites occupy lower slopes than in the active tectonic regions. Despite the overall lower range of slopes, the correspondence of V_S^{30} and slope in stable continental areas suggests that the results there will also be quite useful for site-condition mapping. Analysis of any additional V_S^{30} measurements in stable continental areas that become available will allow us to better quantify the uncertainty as well as establish to what types of geological and geomorphic regimes this methods applies and where it is most limited.

Although these relationships for estimating V_S^{30} are calibrated against a particular resolution topography (30 arc sec global), they hold approximately for both lower- and higher-resolution maps. Beneficial attributes of the topographic-based site-condition maps, in addition to the obvious ease by which they can be produced, include both consistency and spatial continuity of resolution when making V_S^{30} assignments. Unlike geologically based maps, which typically assign a constant velocity to a particular geological unit or units, the topographic-slope approach allows for variable V_S^{30} across a geological unit, characterizing the presumed change in particle size with topographic gradient (alluvial fans or plains, for example). At the same time, with sharp, well-defined topographic features, the ability also exists to show discrete boundaries, for example, at mountain/basin interfaces.

Although the topographic slope approach provides adequate first-order estimates of regional site amplification for the entire globe, there are noted discrepancies. For example, we note a difference in geologically and topographically derived V_S^{30} values between soft and hard rock (NEHRP classes BC and C) and the correlation is made difficult for these units by the lack of V_S measurements. Fortunately, corresponding differences in site amplification for these site classes are relatively small (approximately 25% amplification of bedrock peak ground velocity [PGV] for an input peak ground acceleration [PGA] of 200 cm/sec^2; see Table 1), so distinguishing between them is not as critical as it is for other site classes. Again, additional V_S^{30} data for rock sites should improve our ability to recover V_S^{30} from slope for areas with fast V_S^{30} values. We have also identified some specific geological terraines and processes for which topographic slope and V_S^{30} are unlikely to correlate, and caution is urged in applying our approach without consideration of the geological units and environment. Although we have not made a systematic effort to establish over which geology and erosional and depositional environments our approach is applicable, we anticipate that additional V_S^{30} data acquisition over time will allow us and others to do so. In the mean time, for larger-scale site-condition mapping using higher-resolution topography, additional analysis is required and refined slope ranges will be needed to assign V_S^{30} values.

Empirically based ground motion ShakeMaps produced for earthquakes around the globe benefit from the amplification assigned with this approach. We originally settled on using topography as the base layer for ShakeMap because topography tends to highlight areas of amplified shaking in basins from those less amplified mountainous areas. We had not anticipated the additional benefit of these base maps for constraining the site factors directly.

Topographic gradients can be easily converted to NEHRP site-amplification factors for estimating ground motions in direct conjunction with standard ground-motion prediction equations. In summary, our simple recipe for computing site amplification is thus:

1. Calculate the maximum slope of topography using (GMT command "grdgradient").
2. Determine map extent and compute mean slope over the domain (conveniently, GMT "grdinfo −L2" returns slope mean and standard deviation). For mean slopes less than 0.05, use the stable continent slope ranges for site class assignments; otherwise use the active tectonic slope ranges for site class assignments (Table 2). Alternatively, simply assign Table 2 coefficients based on knowledge of the tectonic regime.
3. Assign V_S^{30} to all sites using the slope and V_S^{30} ranges tabulated in Table 2.
4. For ShakeMap, amplify empirically based ground motions based on the combinations of site class, ground-motion period, and input amplitude based on the Borcherdt (1994) amplification factors given in Table 1 (see Wald *et al.*, 2005, for detailed use in ShakeMap).

In addition to the near-surface site conditions, seismic waves are also known to be strongly influenced by sediment thickness and basin structure (e.g., Frankel *et al.* 1991; Field, 2000). To automatically derive an estimate of soil thickness as well as its shallow velocity, we are investigating the potential for topography to characterize basin structures and their depth. It may also be possible to characterize basins in low, slow regions, by fitting simple functions or shapes (e.g., ellipses) whose aspect ratios should provide an estimate of basin location, orientation, and depth. In the process of analyzing global earthquakes using ShakeMap, we are examining the effects of basin amplification while looking for topographic signatures that might be exploited with routine, uniform processing of globally available data.

We have not fully exploited this topographic slope-based approach for mapping V_S^{30} by using the highest-resolution topographic data available, and this could be done for many areas. In addition, geomorphic, land-use, and other data sets could be brought to bear for some areas where such data exist. Finally, local or regional-scale modifications to the correlations we derived may provide very useful V_S^{30} maps with little additional effort. In areas where numerous V_S^{30} measurements are or become available, minor modifications in the form of an overall static shift to slope-based V_S^{30} predictions or adjustments to the slope versus V_S^{30} correspondence ranges may be warranted.

Acknowledgments

Chris Wills of the California Geological Survey kindly provided his database of V_S^{30} values for California, Ron Street generously compiled and provided his collection of V_S^{30} values for the central United States, Walt Silva provided an early copy of the NGA database, Kris Pankow provided the Utah V_S^{30} data and ShakeMap V_S^{30} grid, Tom Brackman provided Mississippi Embayment regional ShakeMap V_S^{30} grid, and Lisa Hall and Andrew McPherson provided Australian V_S^{30} data. Discussions with Vincent Quitoriano, Chris Wills, Kris Pankow, Lisa Hall, and Andrew McPherson were very beneficial. Reviews by C. Mueller and S. Harmsen, and Associate Editor Ivan Wong improved this manuscript. The maps produced in this analysis were made using Generic Mapping Tools (GMT; Wessel and Smith, 1991). We also appreciate the constructive reviews by Kris Pankow and Chris Wills that led to significant improvements to the manuscript.

References

Ashland, F. X., and G. N. McDonald (2003). Interim map showing shear-wave-velocity characteristics of engineering geologic units in the Salt Lake City, Utah, metropolitan area, Utah Geol. Surv Open-File Report 424, 43 pp.

Bhaduri, B., E. Bright, P. Coleman, and J. Dobson (2002). LandScan: locating people is what matters, *Geoinformatics* **5,** 34–37.

Blatt, H., G. Middleton, and R. Murray (1980). *Origin of Sedimentary Rocks*, Prentice-Hall, Inc., Englewood Cliffs, New Jersey, 767 pp.

Boore, D. M., W. B. Joyner, and T. E. Fumal (1997). Equations for estimating horizontal response spectra and peak accelerations from Western North American earthquakes: a summary of recent work, *Seism. Res. Lett.* **68,** 128–153.

Borcherdt, R. D. (1994). Estimates of site-dependent response spectra for design (methodology and justification), *Earthquake Spectra* **10,** 617–654.

Brackman, T. (2005). ShakeMap implementation for the upper Mississippi Embayment, *M.S. Thesis*, University of Memphis.

Building Seismic Safety Council (BSSC) (2000). National Earthquake Hazards Reduction Program (NEHRP). Part 1: Recommended provisions for seismic regulations for new buildings and other structures, 2000 Edition (FEMA 368), Prepared by the Building Seismic Safety Council for the Federal Emergency Management Agency, Washington, D.C.

Building Seismic Safety Council (BSSC) (2004). NEHRP Recommended provisions for seismic regulations for new buildings and other structures, 2003 edition *(*FEMA 450*)*, Building Seismic Safety Council, National Institute of Building Sciences, Washington, D.C.

Chiou, B. S.-J., and R. R. Youngs (2006). PEER-NGA empirical ground motion model for the average horizontal component of peak acceleration and pseudo-spectral acceleration for spectral periods of 0.01 to 10 seconds, *Interim Report for USGS Review*, 219 pp., http://peer.berkeley.edu/lifelines/repngamodels.html (last accessed December 2006).

Collins, C., R. Kayen, B. Carkin, T. Allen, P. Cummins, and A. McPherson (2006). Shear-wave velocity measurement at Australian ground motion seismometer sites by the spectral analysis of surface waves (SASW) method, presented at *Proc. Aust. Earthquake Eng. Soc. Conf.*, Canberra.

Dhu, T., and T. Jones (Editors) (2002). Earthquake risk in Newcastle and Lake Macquarie, *Geoscience Australia Record 2002/15*, Geoscience Australia, Canberra. http://www.ga.gov.au/urban/projects/archive/newcastle.jsp (last accessed December 2006).

Dobry, R., R. D. Borcherdt, C. B. Crouse, I. M. Idriss, W. B. Joyner, G. R. Martin, M. S. Power, E. E. Rinne, and R. B. Seed (2000). New site coefficients and site classification system used in recent Building Seismic Code provisions, *Earthquake Spectra* **16,** 41–67.

Dobson, J. E., E. A. Bright, P. R. Coleman, R. C. Durfee, and B. A. Worley (2000). LandScan: a global population database for estimating populations at risk, *Photogram. Eng. Remote Sens.* **66,** 849–857.

Farr, T. G., and M. Kobrick (2000). Shuttle Radar Topography Mission produces a wealth of data, *EOS* **81,** 583–585.

Federal Emergency Management Agency (FEMA) 222A (1994). NEHRP recommended provisions for the development of seismic regulations for new buildings, 1994 edition, Part 1: Provisions, Federal Emergency Management Agency, Washington, D.C., 290 pp.

Field, E. H. (2000). A modified ground-motion attenuation relationship for southern California that accounts for detailed site classification and a basin-depth effect, *Bull. Seism. Soc. Am.* **90,** S209–S221.

Frankel, A., S. Hough, P. Friberg, and R. Busby (1991). Observations of Loma Prieta's aftershocks from a dense array in Sunnyvale, California, *Bull. Seism. Soc. Am.* **81,** 1990–1922.

Fumal, T. E., and J. C. Tinsley (1985). Mapping shear-wave velocities of near-surface geologic materials, in J. I. Ziony (Editor), Evaluating earthquake hazards in the Los Angeles region: an earth-science perspective, *U.S. Geol. Surv. Profess. Pap.* **1360,** 101–126.

Gallant, J. C., and T. I. Dowling (2003). A multiresolution index of valley bottom flatness for mapping depositional areas, *Water Resour. Res.* **39,** doi 10.1029/2002WR001426.

Holzer, T. L., A. C. Padovani, M. J. Bennett, T. E. Noce, and J. C. Tinsley, III (2005). Mapping V_S^{30} site classes, *Earthquake Spectra* **21,** 353–370.

Jones, T., M. Middelmann, and N. Corby (editors) (2005). Natural hazard risk in Perth, Western Australia. Canberra, Geoscience Australia, Australian Government. http://www.ga.gov.au/urban/projects/nrap/perth.jsp (last accessed December 2006).

Lee, C.-T., C.-T. Cheng, C.-W. Liao, and Y.-B. Tsai (2001). Site classification of Taiwan free-field strong-motion stations, *Bull. Seism. Soc. Am.* **91,** 1283–1297.

Matsuoka, M, K. Wakamatsu, K. Fujimoto, and S. Midorikawa (2005). Nationwide site amplification zoning using GIS-based Japan Engineering Geomorphologic Classification Map, in *Proc. 9th Int. Conf. on Struct. Safety and Reliability*, 239–246.

Park, S., and S. Elrick (1998). Predictions of shear-wave velocities in southern California using surface geology, *Bull. Seism. Soc. Am.* **88,** 677–685.

Scott, J. B., M. Clark, T. Rennie, A. Pancha, H. Park, and J. N. Louie (2004). A shallow shear-wave velocity transect across the Reno, Nevada, area basin, *Bull. Seism. Soc. Am.* **94,** 2222–2228.

Soller, D. R., and M. C. Reheis (Compilers) (2004). Surficial materials in the conterminous United States, *U.S. Geol. Surv. Open-file Rept. 03-275*, http://pubs.usgs.gov/of/2003/of03-275/ (last accessed March 2007).

Street, R., E. W. Woolery, Z. Wang, and J. B. Harris (2001). NEHRP site classifications for estimating site-dependent seismic coefficients in the Upper Mississippi Embayment, *Eng. Geol.* **62,** 123–135.

Thelen, W., A. M. Clark, C. T. Lopez, C. Loughner, H. Park, J. B. Scott, S. B. Smith, B. Greschke, and J. N. Louie (2006). A transect of 200 shallow shear velocity profiles across the Los Angeles Basin, *Bull. Seism. Soc. Am.* **96,** 1055–1067.

Wald, D. J., V. Quitoriano, T. H. Heaton, H. Kanamori, C. W. Scrivner, and B. C. Worden (1999a). TriNet "ShakeMaps": rapid generation of peak ground-motion and intensity maps for earthquakes in southern California, *Earthquake Spectra* **15,** 537–556.

Wald, D. J., V. Quitoriano, T. H. Heaton, and H. Kanamori (1999b). Relationship between peak ground acceleration, peak ground velocity, and Modified Mercalli Intensity for earthquakes in California, *Earthquake Spectra* **15,** 557–564.

Wald, D. J., B. C. Worden, V. Quitoriano, and K. L. Pankow (2005). ShakeMap Manual: Technical Manual, User's Guide, and Software Guide: U.S. Geological Survey Techniques and Methods, 12A01, 128 pp., http://pubs.usgs.gov/tm/2005/12A01/ (last accessed December 2006).

Wald, D. J., P. S. Earle, K. Lin, V. Quitoriano, and B. Worden (2006). Challenges in rapid ground motion estimation for the prompt assessment of global urban earthquakes, *Bull. Earthquake Res. Inst. Univ. Tokyo* **81,** 275–283.

Wessel, P., and W.H.F. Smith (1991). Generic Mapping Tools, *EOS* **72,** 441.

Wills, C. J., M. D. Petersen, W. A. Bryant, M. S. Reichle, G. J. Saucedo, S. S. Tan, G. C. Taylor, and J. A. Treiman (2000). A site-conditions map for California based on geology and shear wave velocity, *Bull. Seism. Soc. Am.* **90,** S187–S208.

Wills, C. J., and K. B. Clahan (2006). Developing a map of geologically defined site-condition categories for California, *Bull. Seism. Soc. Am.* **96,** 1483–1501.

U.S. Geological Survey
Golden, Colorado 80401
wald@usgs.gov
tallen@usgs.gov

Manuscript received 29 December 2006.